# Influence of the Polymerization Potential on the Transport Properties of Polypyrrole Films

**C. C. Bof Bufon,[†,⊥] T. Heinzel,*[,†] P. Espindola,[‡,§] and J. Heinze[‡,§]**

*Heinrich-Heine-Universität, Universitätsstr. 1, 40225 Düsseldorf, Germany, and Institut für Physikalische Chemie, Albertstr. 21, and Freiburger Materiaforschungszentrum, Stefan Meier Str. 21, Albert-Ludwigs-Universität Freiburg, D-79104 Freiburg, Germany*

*Received: September 4, 2009; Revised Manuscript Received: December 4, 2009*

Polypyrrole films have been prepared by potentiostatic electrochemical polymerization at low temperatures. The cyclic voltammograms and the electronic transport properties of the films are investigated as a function of the polymerization potential. As the potential increases from 520 mV to 1.2 V, the oxidation peak moves to larger voltages, while above 1.2 V, the peak voltage drops again. The film conductivity drops monotonously as the polymerization potential is increased. However, the localization length of the current-carrying states, which characterizes the temperature dependence of the conductivity, correlates with the oxidation peak and shows a minimum for films polymerized at 1.2 V. Furthermore, we show that, with an independent doping step after polymerization, the conductivity of the films can be increased by up to 50%. A maximum conductivity of 1360 S/cm has been observed.

## Introduction

Polypyrrole (PPy)[1] has attracted a lot of attention in recent years since it not only allows studying fundamental questions regarding disordered, semiconductive polymers but also offers a wide range of possible applications. The polymer can be synthesized in water,[2,3] and highly charged PPy films show high conductivities and also stability under ambient conditions.[4−6] Many applications have been demonstrated in the past few years, such as PPy transistors,[7−9] motion,[10] pressure,[11] and gas[12−15] sensing, or detection of bioactivity.[16] In these devices, the PPy film acted as the conductive layer with a conductivity that is modified by the corresponding external signal. PPy has also been used as the active material in actuators, where it responded to an applied voltage by swelling.[17,18] Moreover, PPy compounds have generated recent interest in electrocatalysis aplications.[19−23] For most of these applications, the electronic conductivity $\sigma$ is very important, and it therefore appears essential to be able to adjust it by well-controllable parameters. The conductivity of PPy thin film has been investigated thoroughly in a variety of experiments,[24,25] which discuss, for example, influences such as the polymerization temperature,[4,26] mechanical stretching,[4−6] or aging[27] on $\sigma$. Unfortunately, however, the factors that determine $\sigma$ are not well understood. In comparison to many other conjugated systems like pentacene or poly(hexylthiophene), PPy is strongly disordered, but because of the high doping densities possible, the Fermi energy can be set around the center of the hopping band where the density of states $D(E)$ is high, which results in small hopping distances, and thus relatively large conductivities at room temperature can be achieved. The polymerization potential during potentiostatic growth (or the current in galvanostatic growth, respectively) and also the temperature and the solvent are key parameters for the properties of electrochemically synthesized PPy.[28] It is well-established that as the polymerization temperature and/or the potential is reduced, the films grow at a slower rate while their conductivity increases.[2,29] The reason is that, at higher potentials, higher redox states become accessible for the polymerization process, while at the same time longer chains with a reduced solubility are formed. This is in tune with both cyclic voltammetry and UV/vis spectroscopy, which indicate that, at lower temperatures, the amount of PPy with shorter chain length, also known as PPy II, increases;[30−33] however, the conductivities of pure PPy I and II have not been investigated yet to the best of our knowledge. The surprising finding that films containing more of the short chains show larger conductivities has been attributed to an increased local ordering of the oligomers.[32] Despite these well-known facts, we are not aware of a systematic study regarding the effect of the potential used in potentiostatic growth on the transport properties.

The present work focuses on the influence of the polymerization potential on two characteristic transport parameters, namely, the conductivity $\sigma$ and the localization length $\xi$, which determines the temperature dependence of $\sigma$. We have chosen the polymerization potential $V_p$ as the control parameter since it directly provides an energy scale that is useful for the interpretation of the observations. Our main three findings are as follows: (i) The film conductivity drops monotonously as $V_p$ increases. (ii) The localization length depends nonmonotonously on $V_p$ and has a minimum at $V_p = 1$ V. Its maximum is at 600 mV, only slightly above the lowest potential at which polymerization was possible in our setup, namely, at 520 mV; furthermore, the localization length correlates with the position of the oxidation peak in cyclic voltammograms. (iii) The conductivity of an as-grown film can be further increased by subsequent charging in a monomer-free solution. Here, the maximum conductivity is obtained for polymerization at $V_p =$ 520 mV, followed by an additional charging step at a potential of 600 mV.

* Corresponding author. E-mail: thomas.heinzel@uni-duesseldorf.de. Phone: +49 211 81 14813. Fax: +49 211 81 14266.
† Heinrich-Heine-Universität.
‡ Institut für Physikalische Chemie, Albert-Ludwigs-Universität Freiburg.
§ Freiburger Materiaforschungszentrum, Albert-Ludwigs-Universität Freiburg.
⊥ Present address: Institute for Integrative Nanosciences, IFW Dresden, Helmholtzstr. 20, 01069 Dresden, Germany.

10.1021/jp908565y 
Published on Web 12/18/2009

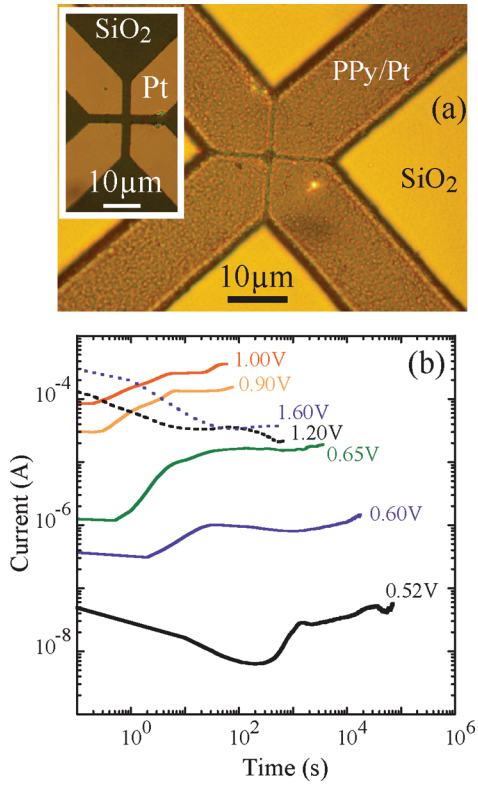


**Figure 1.** (a) Electrode geometry (inset) and sample topography (main figure). In (b), the time dependence of the current during polymerization is shown for some of the polymerization potentials used.

### Sample Preparation and Characterization

Four platinum electrodes of 100 nm thickness were prepared on Si/$SiO_x$ substrates by microlithography as described in detail elsewhere.[32] The lateral distance between the electrodes is 2 $\mu$m; see Figure 1a. The electropolymerization was performed in a conventional electrochemical cell with a standard three-electrode configuration (Metrohm $\mu$-Autolab). The micropatterned Pt electrodes were electrically connected and used in parallel as working electrodes, while an Ag/AgCl wire acted as reference electrode and a Pt plate as counter electrode. It is known that propylene carbonate (PC) not only gives a larger percentage of PPy II in the films compared to other solvents like water or acetonitrile but also has a low freezing point of $-38$ °C and thus allows polymerization at low temperatures. Therefore, the polymerization was carried out in a solution of 0.1 M lithium perchlorate ($LiClO_4$) and 0.5 M Py in PC. The solution was cooled to (243 $\pm$ 0.1) K with an ethanol bath cooler. Potentials smaller than 520 mV were below the activation threshold of the polymerization process, while for potentials above 1.6 V, the solution developed a brown color within seconds, indicating that oligomers are formed in the solution, and the deposition of the electroactive materials stopped. These limiting scenarios therefore define the range of possible polymerization potentials. The duration and amplitude of the applied potential pulse varied between 100 and $10^5$ s, and between +520 mV and 1.6 V, respectively. The electrochemical cell was kept under Ar overpressure during polymerization to avoid oxygen exposure. The PPy film grows at the Pt electrodes which get connected because of lateral growth at a critical film thickness that increases as $V_p$ is increased. Films of about 2 $\mu$m thickness, measured with a scanning force microscope, were prepared at all polymerization potentials.

The film growth rate increased dramatically as $V_p$ is increased, namely, from about 0.5 $\mu$m/day at $V_p = 520$ mV to about 0.5 $\mu$m/min: at $V_p = 1$ V. For potentials higher than 1 V, the solution began to change its color from transparent to a light brown during the polymerization process. This indicates that soluble species (oligomers) are produced in front of the working electrode, which diffuse into solution.

In Figure 1b, the polymerization current $I_p$ as a function of time is shown. Generally, the current depends on the applied potential. It is small for a low oxidation potential but rises by several orders of magnitude as the potential is increased. This gives evidence that the rate of the electrochemical reaction increases with the height of the applied potential pulse. Another characteristic of the pulsed experiments is that the current increases after an initial drop, which proves that the nucleation and growth regime[34] is entered. The time $t_{min}$ after which the minimum current is reached depends strongly on the polymerization potential. As $V_p$ is increased from 520 mV to 1 V, $t_{min}$ drops from 400 to 1 s. For $V_p > 1$ V, however, $I_p$ decreases without a clear signature of an increase at any time before the final film thickness of 2 $\mu$m is reached. This implies that the polymerization process changes its character around $V_p = 1$ V.

Below 1 V, typical electropolymerization processes take place involving nucleation and growth steps after an oligomerization in solution. The long induction periods in the case of pulse potentials between 520 and 650 mV, which are observed before deposition, reveal that, under these conditions, mainly short, soluble, and chainlike oligomers are formed. As has been shown previously, the oligomerization in solution preferably occurs via consecutive "dimerization" steps leading from the starting monomer via a dimer and tetramer to an octamer which then slowly precipitates on the electrode.[32,35,36] During the succeeding growth period they are incorporated into the already deposited material whereas their fraction diminishes as a function of the increasing pulse potential. Simultaneously, under solid-state conditions and again as a function of the applied potential, the oligomeric chains in the film undergo additional coupling steps, leading to the formation of PPy I.

The fact that deposits that have been generated at a formation potential of 520 mV partially dissolve during discharging also proves the existence of short oligomers ($\leq$8 units). Oligomers with chain lengths higher than 8 units are virtually insoluble in PC. Above 1 V, side reactions impede normal oligomerization and deposition steps. It seems that preferably oligomers containing defects are formed, most of which remain in solution. The typical nucleation and growth processes are not observed (Figure 1b). Nevertheless, deposition of electroactive PPy occurs. After deposition at these potentials, cross-linking processes take place (PPy III)[31] that, for example, by $\beta,\beta'$-coupling at the 4- or 5-position of two pyrrole units in different chains slightly increase the effective conjugation length of the material.

At least two samples were grown for each value of a set of polymerization voltages. One of the samples grown at each $V_p$ was characterized by cyclic voltammetry (CV) at room temperature. For this purpose, the samples were immersed in a monomer-free solution of 0.5 M $LiClO_4$ in PC. A constant scan rate of 10 mV/s was used. Further reduction of the scan speed did not modify the shape of the CV traces. Also, we checked the CV traces for various $V_p$ for up to seven samples and found that the main structures discussed below are reproducible.

In Figure 2, the first four voltammetric cycles of a film grown at $V_p = 600$ mV are reproduced. In the first cycle, the reduction peak appears at $-470$ mV and it shifts toward higher potentials in the two subsequent cycles. Oxidation peaks can be seen at 340 and $-240$ mV, indicating the presence of short (PPy II) and longer (PPy I) polypyrrole chains, respectively. Both pyrrole

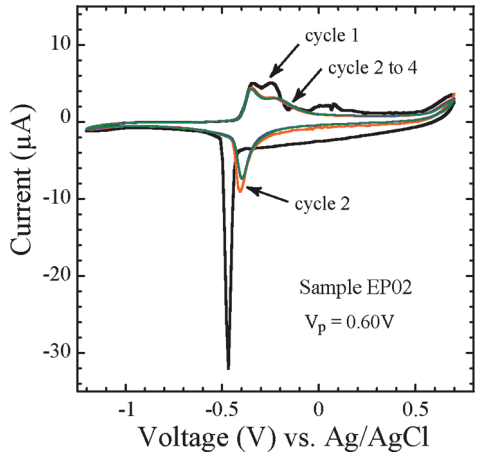


**Figure 2.** Cyclic voltammogram of the PPy film grown at $V_p = 600$ mV. The first four cycles are shown. The structure saturates after three cycles.

species have been identified by UV−vis spectroscopy.[32] It has been established that especially PPy II forms $\sigma$-dimers in the charged state, which induce strong cation incorporation during discharging.[33] Conspicuously, during the very first discharging the reductive charge is significantly higher than that in the following voltammetric cycles. We speculate that this indicates discharging of different types of oligomers, the shortest ones of which probably dissolve. The CVs become stable after the second cycle; a similar behavior is observed for all films, independent of the polymerization potential.

For this we evaluate the data from the fourth cycle, for example, see Figure 3. For better comparability of the peak positions, the currents have been normalized to their maximum value for each trace.

We now turn our attention to the dependence of the oxidation wave on the polymerization potential. As $V_p$ is increased from 600 mV to 1.2 V, the oxidation peaks shift toward more positive voltages and broaden, indicating that, first of all, more PPy I is formed at the expense of PPy II, and second, the distribution of the polymer chain lengths and oxidation energies becomes wider. Despite the fact that the physical chain lengths increase in PPy I, their effective conjugation lengths shorten with increasing formation potentials due to structural defects that are generated during solid-state polymerization. Exceptions are the films grown at $V_p = 520$ mV. Here, the PPy II oxidation peak appears at a larger voltage than for the film grown at $V_p = 600$ mV. This behavior cannot be attributed to a statistical error since we observed it in seven independently grown samples, and the peak voltage in the CV varied by only 7 mV. However, since the polymerization is very slow in this case, the processes may differ. An obvious explanation is that structural peculiarities of a well-ordered material produce an overvoltage effect.

Figure 3b shows the corresponding data for the samples grown between $V_p = 1.2$ V and $V_p = 1.6$ V. Starting at $V_p = 1.2$ V, the oxidation peak begins to shift toward lower potentials as $V_p$ is increased. Additionally, at $V_p = 1.6$ V, the peak width is considerably smaller as compared to lower polymerization potentials. We take this as an indication that, for $V_p \geq 1.2$ V, cross-linking of the deposited oligomers (PPy III)[31] leads to chain segments with improved effective conjugation lengths.

To get better insight into the effective conjugation lengths of the different PPy materials, we followed the approach of Zotti et al., who extracted the number of Py units per oligomer from the maxima in the UV−vis spectra of the neutral material.[37,32] (Figure 4). All the spectra were normalized to an absorbance

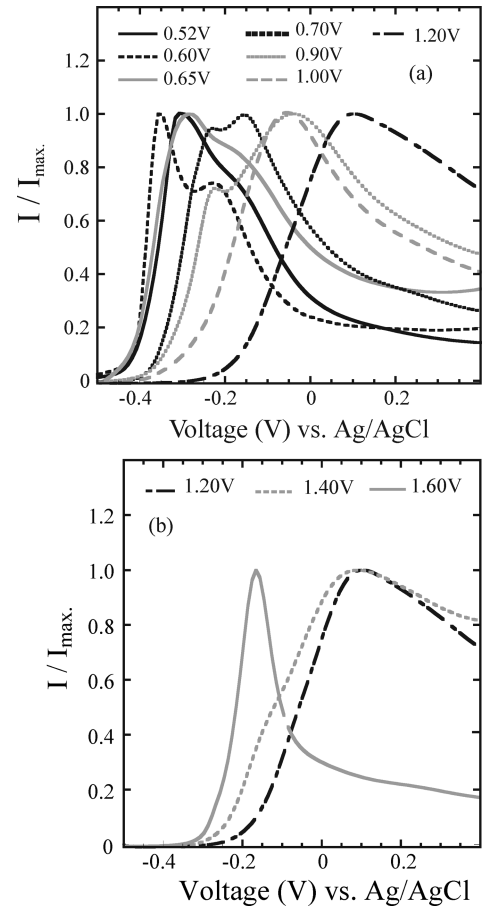


**Figure 3.** Oxidation waves of the PPy films polymerized at low (a) and high (b) potentials $V_p$.

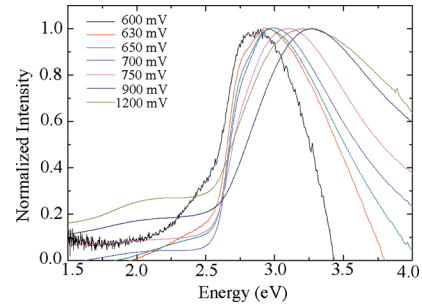


**Figure 4.** UV−vis spectra of PPy films electropolymerized on ITO substrates at potentials between 600 mV and 1.2 V.

of 1. It should be noted that the spectra contain information only about the insoluble deposit. Especially, in the case of films generated between 520 and 650 mV a significant fraction of short oligomers is dissolved during reduction. Thus, the film prepared at a potential of 600 mV preferably shows an absorption band of PPy I, the position of which at 430 nm indicates a chain length between 32 and 64 units. The remaining portion of PPy II that can be detected in CV experiments (chain length of about 12−16 units) is not visible in the UV−vis spectrum because of its low molar absorption coefficient in comparison to that of PPy I. The situation gradually changes at higher formation potentials. The broadening and the shift of the absorption bands to lower wavelengths lead to the following conclusions: (i) at the low wavelength side the absorption of PPy II becomes visible and (ii) the effective conjugation length of PPy I decreases because of the generation of structural defects. However, surprisingly, at formation potentials higher

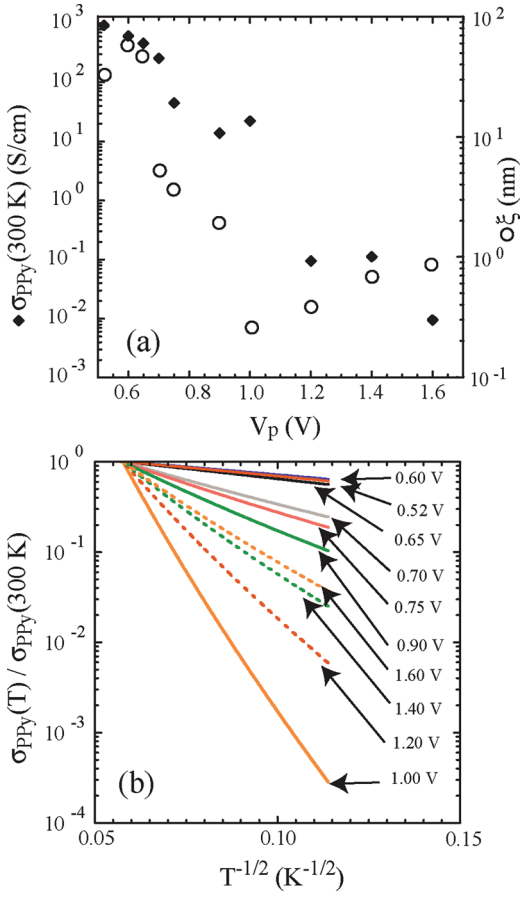


**Figure 5.** (a) Conductivity at room temperature (full squares, left ordinate) and localization length (open circles, right ordinate) of the PPy films as a function of $V_p$. (b) Temperature dependence of the conductivity for several values of $V_p$ as given in the figure, normalized to the conductivity at room temperature. Dashed lines correspond to $V_p > 1$ V and full lines to $V_p \leq 1$ V.

than 900 mV a small shift and broadening to longer wavelengths are observed. This proves that, during electropolymerization, partial chain segments with higher conjugation lengths are formed.

### Transport Experiments

We proceed by discussing the electronic transport properties of the PPy films (Figure 5). The resistances were measured in standard van der Pauw geometry; see Figure 1a. The measurements as a function of temperature were carried out between 85 and 300 K in a Linkam nitrogen cryostat. The conductivity values are obtained from the four-terminal resistance, the film geometry factor, and the film thicknesses which were determined with an atomic force microscope.

As $V_p$ is increased, the conductivity at room temperature gets smaller. In addition, a striking relationship between $V_p$ and the temperature dependence is observed; see Figure 5. As $V_p$ increases 1 V, the conductivity drops strongly, indicating that the films become more insulating. In Figure 5b, it is shown that the logarithm of the conductivity is approximately linear as a function of $T^{-1/2}$, which indicates either Efros-Shklovskii hopping[38] or one-dimensional variable range hopping,[39,40] as observed in many disordered semiconductive films. From these transport experiments, it cannot be distinguished what kind of hopping mechanism is present, but it strikes us as unlikely that the transport in our samples has a strictly one-dimensional character and we therefore assume that the Efros-Shklovskii mechanism is appropriate. We note that while the value of the localization length obtained from different models varies quantitatively, the functional dependence remains the same and thus the following discussion is valid independent of the details of the hopping model applied. Within the Efros-Shklovskii model, the localization length is obtained from a fit of the temperature dependence according to

$$\sigma(T) = \sigma_0 \exp\left[-\left(\frac{T_0}{T}\right)^{1/2}\right] \quad (1)$$

where

$$T_0 = \frac{2.8e^2}{4\pi\varepsilon_0\varepsilon_r k_B \xi} \quad (2)$$

The dependence of $\xi$ on the polymerization potential is shown in Figure 5a as well. At our lowest polymerization potential of $V_p = 520$ mV, the localization length is smaller than that in the sample polymerized at 600 mV, a behavior that correlates with the position of the oxidation peaks (Figure 3). Also, Figure 5a shows that $\xi$ has a minimum at $V_p = 1$ V. Even though for $V_p > 1$ V $\xi$ is a factor of about 50 below its maximum value, it is remarkable that it increases in this regime as $V_p$ is increased. In a disordered system where the current is carried via hopping transport, a hop of a charge carrier can occur only if the initial state is filled, the final state is empty, and both states have an energy within an interval of $k_BT$ around the Fermi energy. The probability for a hopping event is thus not only strongly temperature-dependent but also proportional to the square of the density of states at the Fermi energy $D(E_F)$, which is typically maximum close to the center of the hopping band.[41] Therefore, we can expect that, at a fixed temperature, the prefactor $\sigma_0$ in eq 1, and hence the conductivity, becomes maximum when the hopping band is approximately half-filled. With this in mind, the following picture emerges. The polymerization potential influences both characteristic transport quantities, namely, the filling of the hopping band (i.e., the charge density) via the density of embedded counterions, and the localization length of the states, which depends on the length and local order of the polymer chains. Close to $V_p = 600$ mV, the films show a relatively high structural order. However, the maximum of the density of states of the hopping band resides at lower energies indicated by the increasing conductivity at a smaller localization length as $V_p$ is reduced. When $V_p$ increases to 1 V, the density of states at the Fermi energy drops and the localization length of the states decreases, both of which reduce the conductivity. Increasing $V_p$ further drives the Fermi energy further away from the center of the hopping band, but at the same time the current-carrying states delocalize again.

It is striking and not a priori self-evident that the localization length extracted from the transport data correlates strongly with the conjugation length obtained from the UV−vis spectra. We interpret this as a confirmation of the widely accepted picture that the conjugated $\pi$-bonds that determine the conjugation length form the coherent states that carry the current.

We assume that the $\beta,\beta'$-coupling (cross-linking), indicated by the evolution of the oxidation peak at high polymerization potentials (Figure 3b), increases the conjugation length and thereby supports the delocalization of the states. These two effects, namely, the decreasing density of states and the increasing localization length as $V_p$ increases, influence the conductivity in opposite directions and the measurements reveal

that delocalization of the states dominates in the regime $V_p > 1$ V over the reduction of the density of states at the Fermi level.

Our findings are consistent with the picture that polymerization potential determines both the Fermi energy and the chain length or the structural order, respectively. However, the measurements indicate that these two parameters are not optimized at identical potentials; that is, the potential that maximizes the localization length ($V_p = 600$ mV) differs from the potential for which the band is half-filled ($V_p \leq 520$ mV, as indicated by the conductivity). This raises the question whether $D(E_F)$ and the localization length can be maximized independently, which may lead to an optimization of the conductivity. We recall that, as discussed above, the cycle dependence of the voltammograms indicates a change of both parameters during CV. Therefore, a possible path for obtaining another increase of the conductivity is to grow the films at a potential such that the Fermi energy is as close as possible to the maximum of $D(E)$, and subsequently expose the film to a potential in a pyrrole monomer-free solvent that may induce further charging and increase the localization length, or vice versa. We indeed find that the conductivity can be maximized this way by the following steps: (i) grow the PPy film at $V_p = 520$ mV and (ii) transfer the sample in the monomer-free solution used for CV as described above, increase the potential to $V_p = 600$ mV, and expose them to this potential for 5 min. This procedure increases the room temperature conductivity of the films up to values of about 1360 S/cm, which is, to the best of our knowledge, the highest value reported until now for unstretched PPy films. Another increase of the voltage in the second step leads to a reduction of $\sigma$. In particular, we find $\sigma$ to decline to 825 S/cm for $V_p = 650$ mV and to 493 S/cm for $V_p = 700$ mV. Furthermore, the order of steps (i) and (ii) matters. We did not observe an increase of the conductivity in films grown at $V_p = 600$ mV and subsequent performance of step (ii) at $V_p = 520$ mV. A detailed analysis of this film tuning and the underlying mechanisms, however, requires a thorough experimental characterization of the samples in this narrow parameter regime, which is beyond our scope in the present paper and will be the focus of future experiments.

## Summary and Conclusions

We have presented a systematic study of the influence of the polymerization potential used in potentiostatic growth on the electronic transport properties of polypyrrole films. We find that the conductivity decreases as the polymerization potential is increased. The localization length, however, shows a maximum at a polymerization potential of 600 mV and a minimum at 1 V and correlates with the conjugation length obtained from UV−vis spectroscopy. This behavior is interpreted in terms of the evolution of the electronic structure with the polymerization potential. Within this picture, the density of states of the hopping band has a maximum at an energy that corresponds to a polymerization potential below 520 mV (the lowest possible potential in our setup). The structural order, however, is maximized at a polymerization potential of 600 mV and may indicate a short-range ordering of oligomers. This picture is supported by the fact that the film conductivity can be substantially increased by growing the films at 520 mV and subsequently increasing the doping density by exposing the film to a potential of 600 mV in a monomer-free doping solution. For $V_p > 1$ V, cross-linking takes place, which increases both the localization length and the conjugation length as $V_p$ is increased.

**Acknowledgment.** C.B. and T.H. acknowledge financial support from the Heinrich-Heine University Düsseldorf.

**Supporting Information Available:** This material is available free of charge via the Internet at http://pubs.acs.org.

## References and Notes

(1) *Handbook of Conducting Polymers*, 3rd ed.; Skotheim, T. A., Reynolds, J. R., Eds.; CRC Press/Taylor and Francis: Boca Raton, FL, 2007.
(2) Rodriguez, J.; Grande, H. J.; Cooper, T. F. *Handbook of Organic Conductive Molecules and Polymers*; John Wiley & Sons: New York, 1997.
(3) Simonet, J.; Berthelot, J. R. *Prog. Solid State Chem.* **1991**, *21*, 1.
(4) Ishiguro, T.; Kaneko, H.; Nogami, T.; Ishimoto, H.; Nishiyama, H.; Tsukamoto, J.; Tskahashi, A.; Yamaura, M.; Hagiwara, T.; Sato, K. *Phys. Rev. Lett.* **1992**, *69*, 660.
(5) Sato, K.; Yamamura, T.; Hagiwara, K.; Murata, K.; Tokumoto, M. *Synth. Met.* **1991**, *40*, 35.
(6) Yamamura, M.; Hagiwara, T.; Iwata, K. *Synth. Met.* **1988**, *26*, 209.
(7) Chung, H. J.; Jung, H. H.; Kuk, Y. *Appl. Phys. Lett.* **2005**, *86*, 213113.
(8) Lee, H. J.; Park, S. M. *J. Phys. Chem. B* **2005**, *109*, 13247.
(9) Bof Bufon, C. C.; Heinzel, T. *Appl. Phys. Lett.* **2006**, *89*, 012104.
(10) Dunne, L. E.; Brady, S.; Smyth, B.; Diamond, D. *J. Neuroeng. Rehab.* **2005**, *2*, 4.
(11) Barnoss, S.; Shanak, H.; Bof Bufon, C. C.; Heinzel, T. *Sens. Actuators A* **2009**, *154*, 79.
(12) Miasik, J. J.; Hooper, A.; Tofield, B. C. *J. Chem. Soc., Faraday Trans. 1* **1986**, *82*, 1117.
(13) Hernandez, S. C.; Chaudhuri, D.; Chen, W.; Myung, N. V.; Mulchandani, A. *Electroanalysis* **2007**, *19*, 2125.
(14) Ma, X.; Zhang, X.; Li, Y.; Yu, H.; Li, G.; Wang, M.; Chen, H. *J. Nanopart. Res.* **2008**, *10*, 289.
(15) Al-Mashat, L.; Tran, H. D.; Wlodarski, W.; Kaner, R. B.; Kalantar-Zadeh, K. *IEEE Sensors J.* **2008**, *8*, 365.
(16) Cosnier, S. *Appl. Biochem. Biotechnol.* **2000**, *89*, 127.
(17) Tsai, H.; Xu, H.; Zoval, J.; Madou, M. *Electroactive Polym. Actuators Devices* **2005**, *5759*, 241.
(18) Fujisue, T.; Sendai, T.; Yamato, K.; Takashime, W.; Kaneto, K. *Bioinspir. Biomim.* **2007**, *2*, S1.
(19) Raoof, J.-B.; Ojani, R.; Rashid-Nadimi, S. *Electrochim. Acta* **2004**, *49*, 271.
(20) Zhang, G.; Yang, F. *Electrochim. Acta* **2007**, *52*, 6595.
(21) Zhang, G.; Yang, F.; Gao, M.; Liu, L. *J. Phys. Chem. C* **2008**, *112*, 8957.
(22) Cong, N. H.; El Abbassi, K.; Gautier, J. L.; Chartier, P. *Electrochim. Acta* **2005**, *50*, 1369.
(23) Dong, J.; Hu, Y.; Xu, J.; Qu, X.; Zhao, C. *Electroanalysis* **2009**, *21*, 1792.
(24) Yoon, C. O.; Menon, R.; Moses, D.; Heeger, A. J. *Phys. Rev. B* **1994**, *49*, 10851.
(25) Kohlman, R. S.; Joo, J.; Wang, Y. Z.; Pouget, J. P.; Kaneko, H.; Ishiguro, T.; Epstein, A. J. *Phys. Rev. Lett.* **1995**, *74*, 773.
(26) Lee, K.; Menon, R.; Yoon, C. O.; Heeger, A. J. *Phys. Rev. B* **1995**, *52*, 4779.
(27) Sixou, B.; Mermilliod, N.; Travers, J. P. *Phys. Rev. B* **1996**, *53*, 4509.
(28) Sadki, S.; Schottland, P.; Brodie, N.; Sabouraud, G. *Chem. Soc. Rev.* **2000**, *29*, 283.
(29) Yoon, C. O.; Sung, H. K.; Kim, J. H.; Barsoukov, E.; Kim, J. H.; Lee, H. *Synth. Met.* **1999**, *99*, 201.
(30) Zhou, M.; Heinze, J. *Electrochim. Acta* **1999**, *44*, 1733.
(31) Zhou, M.; Heinze, J. *J. Phys. Chem. B* **1999**, *103*, 8443.
(32) Bof Bufon, C. C.; Vollmer, J.; Heinzel, T.; Espindola, P.; John, H.; Heinze, J. *J. Phys. Chem. B* **2005**, *109*, 19191.
(33) Zhou, M.; Pagels, M.; Geschke, B.; Heinze, J. *J. Phys. Chem. B* **2002**, *106*, 10065.
(34) Downard, A. J.; Pletcher, D. *J. Electroanal. Chem.* **1986**, *206*, 147.
(35) Smie, A.; Synowczyk, A.; Heinze, J.; Alle, R.; Tschuncky, P.; Götz, G.; Bäuerle, P. *J. Electroanal. Chem.* **1998**, *452*, 87.
(36) Heinze, J. In *Organic Electrochemistry*, 4th ed.; Lund, H., Hammerich, O., Eds.; Marcel Dekker: New York, 2000; Chapter *32*, p 1309.
(37) Zotti, G.; Berlin, A.; Pagani, G.; Schiavon, G.; Zecchin, S. *Adv. Mater.* **1993**, *6*, 231.
(38) Efros, A. L.; Shklovskii, B. I. *J. Phys. C* **1975**, *8*, L49.
(39) Mott, N. F. *Metal Insulator Transitions*; Taylor and Francis: London, 1974.
(40) Mott, N. F.; Kaveh, M. *Adv. Phys.* **1985**, *34*, 329.
(41) Ambegaokar, V.; Halperin, B. I.; Lange, J. S. *Phys. Rev. B* **1971**, *4*, 2612.

JP908565Y